Future Generation Computer Systems 87 (2018) 152–158

Contents lists available at ScienceDirect

Future Generation Computer Systems

journal homepage: www.elsevier.com/locate/fgcs

Heterogeneous 3-D ICs as a platform for hybrid energy harvesting in IoT systems☆

Boris Vaisband [a,*,1], Eby G. Friedman [b,2]

[a] Department of Electrical and Computer Engineering, University of California, Los Angeles, CA 90095, USA
[b] Department of Electrical and Computer Engineering, University of Rochester, Rochester, NY 14627, USA

ARTICLE INFO

Article history:
Received 25 September 2017
Received in revised form 6 April 2018
Accepted 29 April 2018
Available online 12 May 2018

Keywords:
3-D IC
Internet of things
Hybrid energy harvesting
Heterogeneous integration

ABSTRACT

Three-dimensional integrated circuits are a natural platform for IoT systems. IoT systems exhibit a small footprint, integrate disparate technologies, and require long term sustainability (extremely low power or self-powered). A hybrid energy harvesting system within a three-dimensional integrated circuit is proposed in this paper. The harvesting system exploits different types of energy available from the ambient (electromagnetic, solar, thermal, and kinetic). Integration of the hybrid harvesting system onto a three-dimensional platform ensures that each type of harvested energy can be individually collected. Both static and dynamic evaluations of a hybrid energy harvesting system are provided. For an example IoT system, the static power requirements are approximately 85% of the power delivered to the load. In the dynamic evaluation, a range of activity factors characterizing the load and different storage capacitors are considered. The power requirements of a typical IoT system are shown to be satisfied by a hybrid energy harvesting system within a 3-D platform.

1. Introduction

The Internet of Things (IoT) is a novel computing paradigm based on connecting physical devices to the global network. IoT devices typically exhibit the following characteristics [1]: (1) small physical dimensions, (2) communications (typically wireless) capability, (3) sensing/actuation modality, and (4) low energy consumption. In addition to these key characteristics, IoT devices often operate in extreme environments, such as automotive engines, smart homes, industrial facilities, home appliances, and corrosive surroundings such as within or on the human body. IoT devices need to withstand hostile environments such as increased and highly variable temperatures, liquid immersion, and significant vibration.

Three-dimensional (3-D) integrated circuits (ICs) are a platform for heterogeneous integration, and exhibit a small form factor [2]. These traits of 3-D ICs make 3-D integration a natural platform for IoT devices [3]. The disparate technologies of IoT devices, including MEMS sensors and actuators, RF and wireless communication, energy harvesting circuitry, and computational logic, can be integrated as individual layers within a 3-D structure. Interface circuits efficiently communicate from the IoT sensors to the relevant layer(s) within a 3-D IC, and from the on-chip controllers within a 3-D system to the IoT actuators.

The layers within a 3-D IC are connected by through substrate vias (TSVs) [4]. The TSVs are short vertical interconnections (typically 20 μm in length and 2 to 4 μm in diameter [2]) that carry a variety of signals (power, clock, and data) between different layers within a 3-D IC.

IoT devices are typically intended to be self-powered [5,6]. Some low cost and easily accessible devices can be replaced when the battery becomes depleted; however, other devices are dependent on alternative forms of energy to prolong lifetime. Four basic forms of energy exist in the ambient [7], (1) electromagnetic (EM), (2) solar, (3) thermal, and (4) kinetic. The most common energy harvesting circuits target solar and electromagnetic energy. It has been experimentally shown that the ambient exhibits EM power densities of 0.1 to 1 μW/cm^2 [8]. The available solar power density in the ambient is on the order of mW when illuminated using the standard global solar irradiance spectrum [9]. The magnitude of the harvested thermal power, using a thermoelectric generator (TEG), and kinetic power, using a piezoelectric device is, respectively, 0.52 mW and 8.4 mW [7]. The different types of energy in the

☆ This research is supported in part by the Ministry of Education, academic research fund (AcRF), TIER 2, Singapore under Grant No. MOE2014-T2-2-105, the National Science Foundation, United States under Grant Nos. CCF-1329374 and CCF-1526466, IARPA, United States under Grant No. W911NF-14-C-0089, AIM Photonics, United States under Award No. 059447-007, the Intel Collaborative Research Institute for Computational Intelligence (ICRI-CI), United States, and by grants from Cisco Systems and Qualcomm, United States.

* Corresponding author.
E-mail addresses: vaisband@ucla.edu (B. Vaisband), friedman@ece.rochester.edu (E.G. Friedman).
[1] Member, IEEE.
[2] Fellow, IEEE.

https://doi.org/10.1016/j.future.2018.04.092
0167-739X/

Table 1
Typical harvested power for different energy types available from the ambient [7–9].

Energy type	Harvested power
EM	0.1 to 1 μW
Solar	1 to 10 mW
Thermal	0.52 mW
Kinetic	8.4 mW

ambient and the range of harvested power are summarized in Table 1.

Hybrid energy harvesting circuits have recently been developed for solar and EM energy [10]. The 3-D platform, however, can integrate available energy harvesting methods within a single structure. In addition to harvesting multiple sources of energy (solar, EM, thermal, and kinetic, see Fig. 1), the power efficiency of delivering harvested power to the load in 3-D ICs is higher than in conventional two-dimensional (2-D) ICs. Each energy harvesting circuit benefits from different substrate materials. For example, efficient solar cells have been demonstrated on a PET substrate [11], while thermoelectric circuits are commercially available using a Bi_2Te_3 substrate [12]. Several energy harvesting and management techniques for powering IoT devices, applicable to any type of harvested energy, have also been proposed [13]. The 3-D platform supports the integration of these heterogeneous substrates within a single, small platform.

Communications circuits typically consume significant power to transmit data. The power overhead occurs when initializing the transmitter. To lower this power overhead, memory arrays are sometimes included within the IoT devices. The data are stored in memory and transmitted at a later time when a sufficient amount of data has been accumulated. Advanced memory technologies can also be integrated within a 3-D IC, exploiting ferromagnetic substrate materials and the short distance to the computational layer.

The rest of the paper is composed of the following sections. Common IoT circuits and substrate materials are reviewed in Section 2. A hybrid energy harvesting system within a 3-D platform is described in Section 3. An evaluation of the power efficiency of a hybrid 3-D IoT system from both a static and dynamic perspective is discussed in Section 4. Some conclusions are offered in Section 5.

2. Common IoT circuits and substrate types

Each layer in a 3-D IC is individually fabricated using a process optimized for that application [2]. Different substrate materials are compatible with different circuits. The electrical, thermal, mechanical, and optical properties of certain substrate materials used in common ICs for IoT devices are listed in Table 2.

Each of the substrate materials listed in Table 2 is beneficial for a certain type of circuit. Silicon (Si) is lower cost and technologically more mature than the other materials listed in Table 2, and is therefore used for mainstream, high complexity processor and memory applications. Polyethylene terephthalate (PET) is low cost and provides high transparency [11]. PET is used as the substrate of p-i-n type solar cells and is compatible with traditional deposition processes of solar cells on glass substrates [11]. Thermoelectric generators (TEG) typically consist of multiple pairs of p-type and n-type bismuth telluride (Bi_2Te_3) thermoelectric structures, which produce electrical energy by exploiting temperature gradients between the hot surface (human body) and the cold surface (ambient air) [12,14]. Aluminum nitride (AlN) is commonly used for piezoelectric devices as this material can be processed by CMOS compatible technologies at low temperature (200 °C to 400 °C). AlN also exhibits higher phase velocity and a moderately high piezoelectric coefficient than other piezoelectric materials (*e.g.*, GaN and ZnO) [15]. Piezoelectric sensors can harvest kinetic energy from the ambient. This energy originates from vibrations and other physical movement. Piezoelectric sensors capture and transform these motions into electrical energy. The superior electron mobility and direct bandgap of gallium arsenide (GaAs) makes GaAs attractive for certain high performance digital, analog, and optical applications. Germanium (Ge) is also a favorable substrate material for photovoltaic and photodetector systems due to the high absorption coefficient of Ge. Military and space application that require high quality infrared detectors commonly use mercury cadmium telluride (HgCdTe) which has a tunable bandgap ranging from 0.1 eV to 1 eV [16]. This property of HgCdTe supports detection of long wavelengths of light. Each of these technologies can support a variety of IoT applications while comfortably fitting into a single 3-D system.

Several semi-hybrid energy harvesting approaches have been considered in recent years, exhibiting the benefits of heterogeneous integration. In [10], a combination of EM and solar energy harvesters is demonstrated. In this work, a flexible photovoltaic film is placed on the metal and arranged to increase the efficiency of the EM harvesting antenna. Another semi-hybrid energy scheme is proposed in [17]. In this work, a combination of solar and kinetic energy is demonstrated on-chip, fabricated using a UMC 0.18 μm bipolar-CMOS-DMOS process. The two primary contributions in this work are (1) a constant voltage method to balance power conversion efficiency against circuit complexity to process the light energy, and (2) an on-chip bridge rectifier to handle the AC signal generated by the vibration energy. Similar fabrication approaches to those methods described in [10] and [17] can be utilized within a 3-D IC platform to enable a hybrid integration of several types of energy harvesters. Furthermore, the 3-D platform simplifies heterogeneous integration since various materials (as described in the beginning of this section), processes (*e.g.*, UMC 0.18 μm bipolar-CMOS-DMOS), and types of circuits (*i.e.*, for DC and AC energy) can coexist in 3-D ICs.

Table 2
Common circuit applications and compatible substrate types.

Applications	Substrate materials	Electrical resistivity Ω · cm	Thermal conductivity W/(m°K)	Refractive index	Young's modulus GPa	Thermal expansion coefficient at 300° 10^{-6}/°K	Wavelength range nm
Processor/memory	Silicon (Si)	1 to 10	138	3.4 to 3.5	130 to 185	2.6	400 to 1,060
Solar cells	Polyethylene Terephthalate (PET)	$1 \cdot 10^{16}$	0.2	1.6	2 to 2.7	3.9	400 to 1,600
Thermoelectric	Bismuth Telluride (Bi_2Te_3)	$0.6 \cdot 10^{-3}$	1.2	9.2	50 to 55	1.3	400 to 2,500
Piezoelectric	Aluminum Nitride (AlN)	$1 \cdot 10^{14}$	140 to 180	1.9 to 2.2	308	5.27	1,000 to 1,500
RF/analog	Gallium Arsenide (GaAs)	$4 \cdot 10^{7}$	40	3.9	85.9	6.86	650 to 870
Photonics	Germanium (Ge)	$1 \cdot 10^{-3}$	45	4 to 4.1	102.7	5.8	600 to 1,600
Space/detectors	Mercury Cadmium Telluride (HgCdTe)	2	0.2	4	42 to 48	4.7	2,000 to 5,400

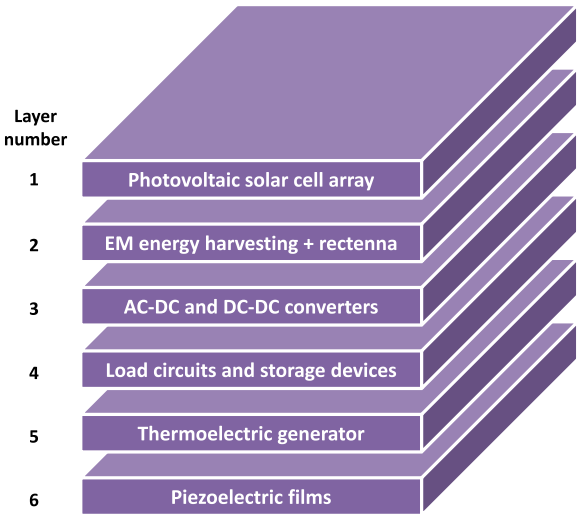

Fig. 1. Proposed hybrid harvesting 3-D system.

3. Hybrid harvesting system within a 3-D platform

The topology of the proposed hybrid energy harvesting system within a 3-D platform is shown in Fig. 1. Each layer of the 3-D IC consists of an individual substrate material, fabricated using a process optimized for that technology. The layers are interconnected using TSVs to create short low impedance interconnections between the layers. Low power dissipation is a key objective for IoT devices, therefore a 3-D structure, as illustrated in Fig. 1, with short vertical interconnections is highly desirable.

The proposed system consists of energy harvesting mechanisms for each type of ambient energy. For harvesting solar energy, on-chip solar cells (*e.g.*, photodiodes) are integrated on layer 1. The harvested DC power is directed to the conversion layer (layer 3) with TSVs. Two sets of stacked TSVs deliver power to the conversion layer with a total vertical interconnect length of ~ 40 μm. To harvest EM energy, an on-chip rectifying antenna (rectenna) is placed on layer 2 of the hybrid 3-D system. The harvested DC power is transferred with TSVs on layer 3 and, if necessary, converted to a different voltage level. A TEG is placed on layer 5 of the harvesting system (see Fig. 1). The TEG is an on-chip DC voltage source [18]; power conversion is therefore not required. The TEG-based voltage sources supply current to the load circuits on layer 4 of the 3-D system. Piezoelectric films are deposited on layer 6 of the hybrid harvesting structure. AC power is delivered to layer 3 and converted to DC using AC-to-DC converters placed on this layer.

On-chip converters [19] are utilized within the conversion system on layer 3 of the 3-D system. These converters typically exhibit a high conversion efficiency (above 99%) due to low parasitic impedances. Integrating the harvesting mechanisms (solar cells, rectenna, TEG, piezoelectric films) onto a 3-D platform increases the efficiency of the overall system by reducing the parasitic impedances.

The energy available from the ambient is typically scarce, therefore integrating harvesting circuits that exploit multiple types of energy sources within a single system is an effective approach. In a hybrid system, power is simultaneously harvested from the different sources depending upon the availability of each type of energy. Since the availability of the different energies is inconsistent (*e.g.*, no solar energy during cloudy days or at night, or no kinetic energy when stationary), certain harvesting systems may be turned off (sleep mode) while other systems continue to harvest available energy. This feature reduces leakage power in non-utilized systems while harvesting power when the energy is available.

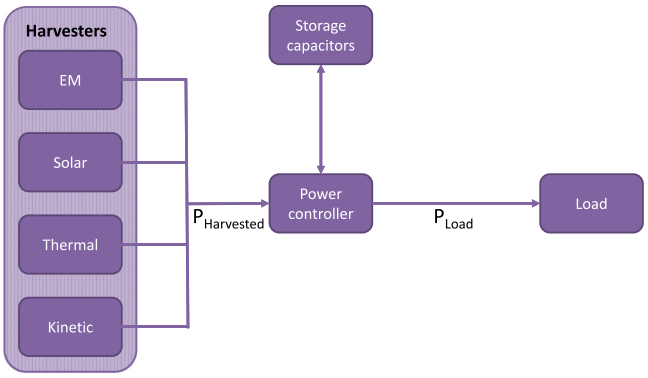

Fig. 2. Block diagram of energy harvesting and power delivery system. The storage capacitors are used to retain excess power.

Table 3
Experimental efficiency of on-chip harvesting systems and energy availability due to environmental conditions.

Energy type	Efficiency η	Availability α
Electromagnetic	2%	100%
Solar	59%	15%
Thermal	0.15%	80%
Kinetic	91%	5%

4. Hybrid energy harvesting for IoT systems

A block diagram of the power delivery system is shown in Fig. 2. The system consists of four dedicated energy harvesters, a power controller, storage device, and the load. The amount of power harvested from the ambient $P_{Harvested}$ is strongly dependent upon the availability of the harvested energy, and the efficiency of the harvesting mechanism and power delivery system, as described in Section 4.1. The harvested power is converted and delivered to either the load or on-chip capacitive storage devices (*e.g.*, micro-supercapacitors [20]). In certain harvesting mechanisms, as described in Section 3, only DC–DC conversion or no conversion is required. The hybrid energy harvesting system is evaluated in Sections 4.2 and 4.3.

The power controller is responsible for managing the harvested power and the storage capacitors. The following methodology is used when transferring power to and from the storage capacitors:

if $(P_{Harvested} > P_{Load})$ ***then*** charge capacitors
if $(P_{Harvested} < P_{Load})$ ***then*** discharge capacitors
if $(P_{Harvested} = P_{Load})$ ***then*** do nothing

The load is supplied by either the harvested or stored power, according to the availability of the ambient energy. In certain cases, if power is unavailable in both the ambient and storage capacitors, the power controller will activate a sleep mode state until additional power is available. The efficiency and availability of power are discussed in Section 4.1. A static and dynamic evaluation of a hybrid energy harvesting system is provided in, respectively, Sections 4.2 and 4.3.

4.1. Efficiency and availability of power

The power efficiency (η) of each on-chip harvesting system, including conversion and delivery of power, is summarized in Table 3. Piezoelectric films and solar cells exhibit high harvesting efficiencies, respectively, 91% and 59% [21,22]. The high harvesting efficiency combined with the available ambient power (see Table 1) makes these two sources of energy highly desirable. Piezoelectric energy is typically scarce when stationary since vibrations are required by the piezoelectric harvesting system.

Alternatively, EM and thermal energy are typically always available although at significantly lower levels. The harvesting efficiency of the on-chip rectennas and TEG devices is low, respectively, 2% and 0.15% [23,24]. Power delivery techniques are required to combine the harvested energy and distribute the generated voltages across a 3-D IC.

In addition to the efficiency of harvesting, conversion, and delivery of power, environmental conditions significantly affect the availability of each type of energy within the ambient, as described in Section 3. The availability due to environmental conditions α for each type of energy is summarized in Table 3.

The total power delivered to the load using a hybrid harvesting system is

$$P_{\text{delivered}}^{\text{total}} = P_{\text{delivered}}^{\text{EM}} + P_{\text{delivered}}^{\text{solar}} + P_{\text{delivered}}^{\text{thermal}} + P_{\text{delivered}}^{\text{piezo}} \ , \tag{1}$$

where $P_{\text{delivered}}^{\text{total}}$ is the total power delivered to the load and is the sum of the power harvested by each type of harvesting mechanism. Each harvesting system delivers power according to

$$P_{\text{delivered}} = \alpha P_{\text{ambient}} \cdot \eta \ . \tag{2}$$

4.2. Static evaluation of hybrid harvesting system

A static evaluation of the delivered power assumes that the load requires maximum power. The total harvested power is determined according to the available power in the ambient (Table 1) and the efficiency of the power harvesting and delivery system (Table 3). In addition, the availability of each type of power due to environmental conditions is determined according to α (see Table 3).

The delivered power for each type of ambient energy is

$$P_{\text{delivered}}^{\text{EM}} = \alpha^{\text{EM}} \cdot P_{\text{harvested}}^{\text{EM}} \cdot \eta^{\text{EM}} = 1 \cdot 0.55\ \mu\text{W} \cdot 0.02 = 0.011\ \mu\text{W} \tag{3}$$

$$P_{\text{delivered}}^{\text{solar}} = \alpha^{\text{solar}} \cdot P_{\text{harvested}}^{\text{solar}} \cdot \eta^{\text{solar}} = 0.15 \cdot 5.5\ \text{mW} \cdot 0.59 = 0.49\ \text{mW} \tag{4}$$

$$P_{\text{delivered}}^{\text{thermal}} = \alpha^{\text{thermal}} \cdot P_{\text{harvested}}^{\text{thermal}} \cdot \eta^{\text{thermal}} = 0.8 \cdot 0.52\ \text{mW} \cdot 0.15 = 0.062\ \text{mW} \tag{5}$$

$$P_{\text{delivered}}^{\text{piezo}} = \alpha^{\text{piezo}} \cdot P_{\text{harvested}}^{\text{piezo}} \cdot \eta^{\text{piezo}} = 0.05 \cdot 8.4\ \text{mW} \cdot 0.91 = 0.38\ \text{mW} \tag{6}$$

resulting in a total delivered power,

$$P_{\text{delivered}}^{\text{total}} = 0.011\ \mu\text{W} + 0.49\ \text{mW} + 0.062\ \text{mW} + 0.38\ \text{mW} = 0.94\ \text{mW} \ . \tag{7}$$

Assuming an ultra-low power supply voltage V_{DD} = 0.5 volts and a maximum load current I_{max} = 1.6 mA required for sensing, computation, and communication within an IoT device [25], the maximum required power is

$$P_{\text{required}} = V_{DD} \cdot I_{max} = 0.5\ \text{V} \cdot 1.6\ \text{mA} = 0.8\ \text{mW} \ , \tag{8}$$

approximately 85% of the available power.

4.3. Dynamic evaluation of hybrid harvesting system

The static evaluation only provides a snapshot of the power delivered to the load by the hybrid harvesting system under specific conditions. A dynamic evaluation is therefore required to include temporal conditions of both the harvesting system and the load. The hybrid energy harvesting system has been evaluated over a 24 h period. Similar to the static evaluation, an IoT system with V_{DD} = 0.5 volts and a maximum current consumption of I_{max} = 1.6 mA is assumed. The load activity is randomly generated according to the activity factor (which determines when the load consumes current).

An evaluation of the power harvested by the hybrid harvesting system is depicted in Figs. 3, 4, and 5. The total harvested power, load power, and storage power are each depicted in Figs. 3, 4, and 5. Similar to the static evaluation, the total harvested power is determined according to the available power in the ambient (see Table 1), and the efficiency (η) and availability (α) characteristics (see Table 3).

The information shown in Figs. 3, 4, and 5 follow the power transfer methodology (see Section 4). When the harvested power is larger than the power required by the load, the excess charge is transferred to the storage capacitors. The charge stored by the capacitors increases until the capacitors are full; any additional excess power is lost. If the harvested power is smaller than the power required by the load, additional charge is transferred from the storage capacitors to the load.

In Fig. 3, an activity factor of 0.5 is applied to the load while the magnitude of the storage capacitors is 33 mF. Note that the harvested energy is insufficient during the night when solar energy is not available. The power of the storage capacitors becomes negative. Negative charge on the storage capacitors identifies the time when the harvested and stored power is insufficient to supply the power requirements of the load. In Fig. 4, the activity factor of the load is reduced from 0.5 to 0.3, and similar storage capacitors are used. Both fewer and smaller negative events are exhibited for the storage capacitors, indicating that the hybrid harvesting system is better capable of supplying the power requirements of the load. To emphasize the flexibility of the 3-D platform, a larger capacitor has been evaluated, as shown in Fig. 5, along with a lower activity factor (0.1). Note that the hybrid harvesting system can supply all of the power requirements of the load with an activity factor of 0.1 while supported by storage capacitors of 66 mF.

This evaluation suggests a large design space where multiple techniques exist to support the power requirements of IoT systems. The storage capacitors can be increased at the expense of additional layers within the 3-D platform, the activity factor of the load can be dynamically adjusted, multiple system states can be exploited (*e.g.*, sleep state), and data transmission protocols can be utilized to save power.

5. Conclusions

3-D ICs are a natural platform for IoT devices. 3-D ICs provide a platform for heterogeneous integration of the disparate technologies required for IoT systems, including different substrate materials and unique processing of individual layers. The 3-D platform also provides the small form factor necessary for small IoT devices. In addition, improved power efficiency is exhibited due to smaller parasitic interconnect impedances.

The 3-D structure provides opportunities for self-sustainability of IoT devices. Hybrid power harvesting of all four energy forms available in the ambient is supported by the 3-D structure, leading to self-sustainable, miniature, and intelligent systems. The different harvesting circuits can be integrated onto different layers within a 3-D structure. The primary benefit of a hybrid harvesting system is the increased energy available from individually scarce and inconsistent sources of energy.

Both static and dynamic evaluation of the hybrid energy has been performed. The static evaluation verifies that the harvesting system is able to supply a load at maximum power requirements. The static power is approximately 15% higher than the power required by the load for the evaluated system. The dynamic evaluation includes the temporal behavior of both the hybrid harvesting

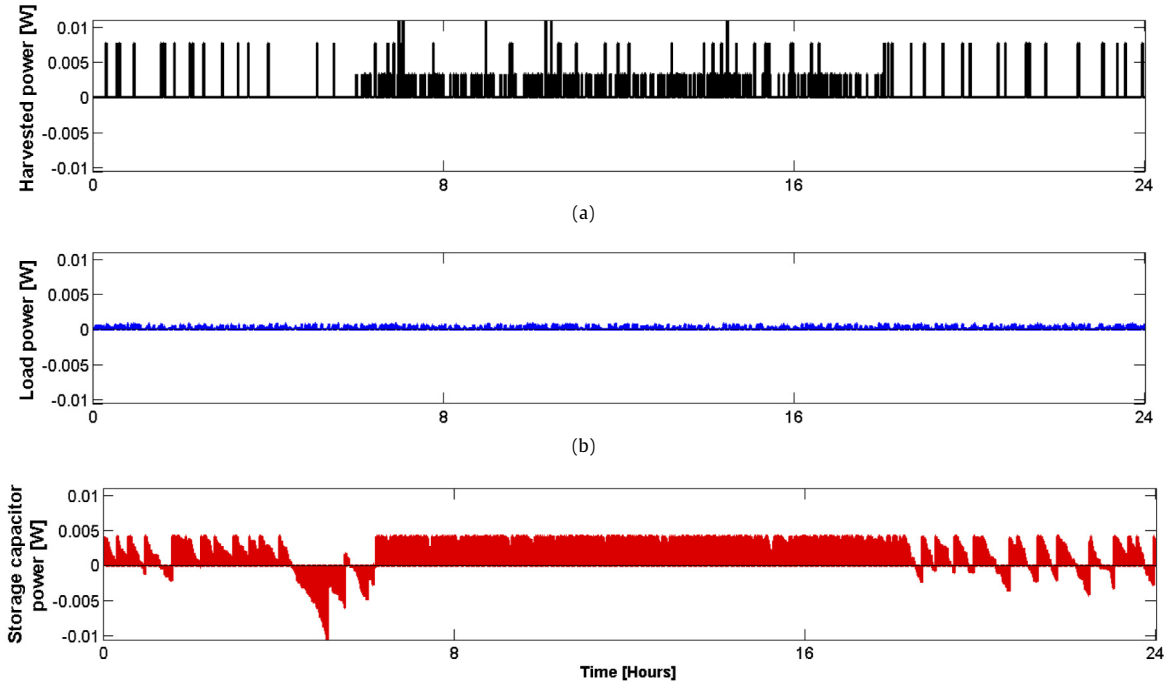

Fig. 3. Evaluation of hybrid energy harvesting system with a load activity factor of 0.5 and a storage capacitor of 33 mF. (a) Harvested power, (b) load power, and (c) storage capacitor power.

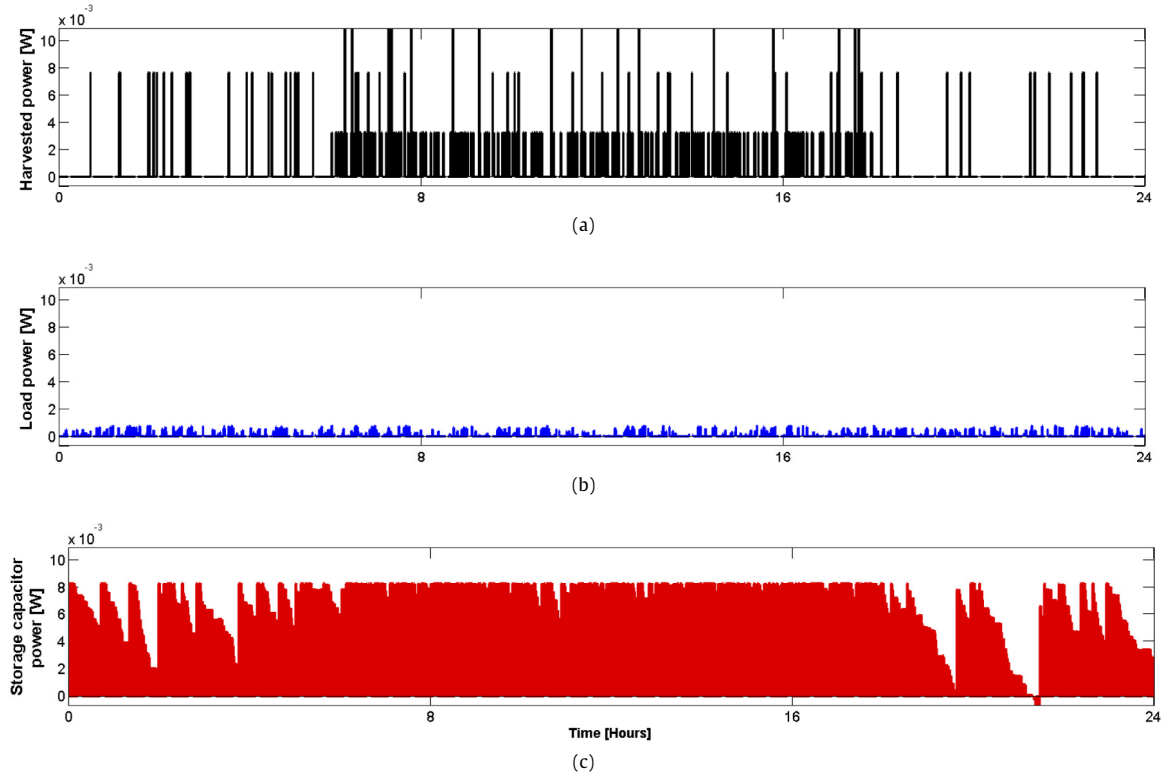

Fig. 4. Evaluation of hybrid energy harvesting system with a load activity factor of 0.3 and a storage capacitor of 33 mF. (a) Harvested power, (b) load power, and (c) storage capacitor power.

system and the load. The power requirements of the load can be satisfied by adjusting certain parameters (*e.g.*, size of capacitive storage) based on the environmental conditions of the application (*e.g.*, availability of solar energy). In addition, the power controller can be configured to change the operating state of the IoT system to accommodate the available power budget.

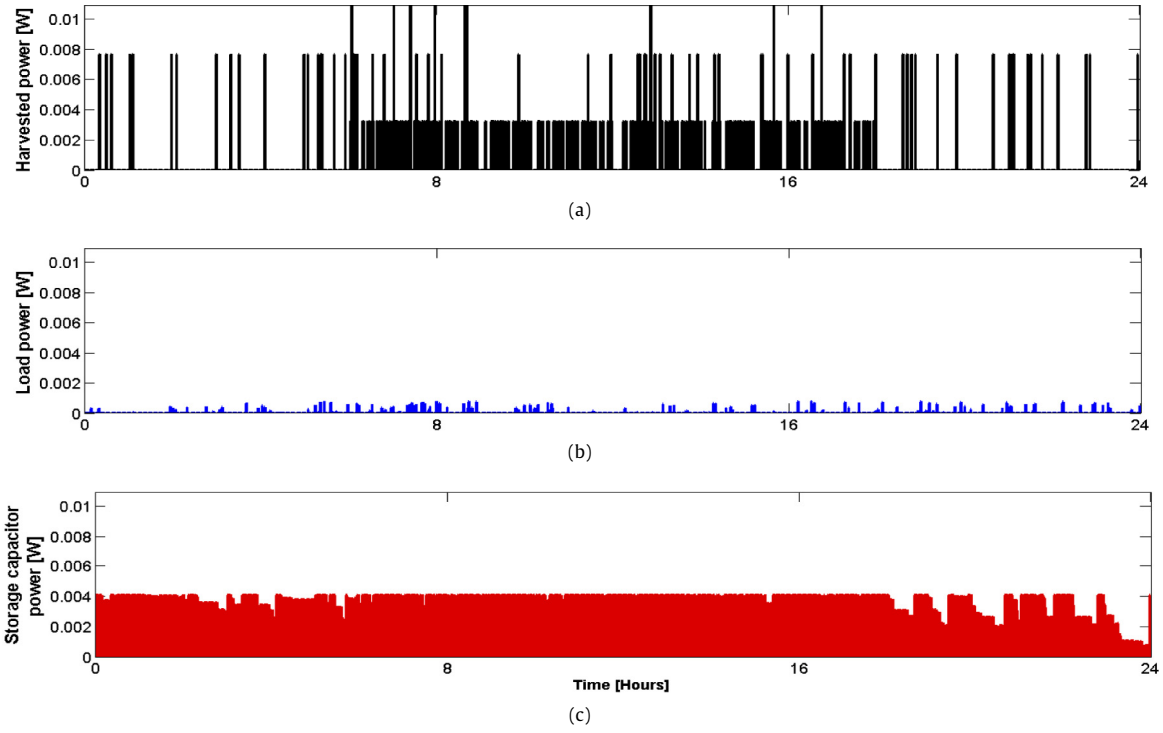

Fig. 5. Evaluation of hybrid energy harvesting system with a load activity factor of 0.1 and a storage capacitor of 66 mF. (a) Harvested power, (b) load power, and (c) storage capacitor power.

References

[1] D. Blaauw, D. Sylvester, P. Dutta, Y. Lee, I. Lee, S. Bang, Y. Kim, G. Kim, P. Pannuto, Y.S. Kuo, D. Yoon, W. Jung, Z. Foo, Y.P. Chen, S. Oh, S. Jeong, M. Choi, IoT design space challenges: Circuits and systems, in: Proceedings of the IEEE Symposium on VLSI Technology, 2014, pp. 1–2.

[2] V.F. Pavlidis, E.G. Friedman, Three-Dimensional Integrated Circuit Design, Morgan Kaufmann, 2009.

[3] B. Vaisband, E.G. Friedman, Hybrid energy harvesting in 3-D IC IoT devices, in: Proceedings of the IEEE International Symposium on Circuits and Systems, 2017, pp. 2573–2576.

[4] B. Vaisband, E.G. Friedman, Noise coupling models in heterogeneous 3-D ICs, IEEE Trans. Very Large Scale Integr. (VLSI) Syst. 24 (8) (2016) 2778–2786.

[5] K.Z. Ahmed, M. Kar, S. Mukhopadhyay, (Invited Paper) Energy delivery for self-powered IoT devices, in: Proceedings of the IEEE/ACM Asia and South Pacific Design Automation Conference, 2016, pp. 302–307.

[6] H. Jayakumar, K. Lee, W.S. Lee, A. Raha, Y. Kim, V. Raghunathan, Powering the Internet of Things, in: Proceedings of the IEEE/ACM International Symposium on Low Power Electronics and Design, 2014, pp. 375–380.

[7] A. Georgiadis, Energy harvesting for autonomous wireless sensors and RFID's, in: Proceedings of the IEEE General Assembly and Scientific Symposium, 2014, pp. 1–5.

[8] H.J. Visser, A.C.F. Reniers, J.A.C. Theeuwes, Ambient RF energy scavenging: GSM and WLAN power density measurements, in: Proceedings of the IEEE European Microwave Conference, 2008, pp. 721–724.

[9] D.G. Collins, W.G. Blattner, M.B. Wells, H.G. Horak, Backward Monte Carlo calculations of polarization characteristics of the radiation emerging from spherical shell atmospheres, Appl. Opt. 11 (11) (1972) 2684–2696.

[10] I.J. Hwang, D. Kwon, D.J. Lee, J.W. Yu, W.S. Lee, EM/light hybrid energy harvesting with directional dipole antenna for IoT sensor, in: Proceedings of the IEEE Antennas and Propagation Society International Symposium, 2015, pp. 1292–1293.

[11] J. Ni, J. Zhang, J. Xue, X. Wang, L. Cao, C. Wu, S. Xiong, X. Geng, Y. Zhao, Effect of pretreatment on PET films and its application for flexible amorphous silicon solar cells, in: Proceedings of the IEEE Photovoltaic Specialists Conference, 2009, pp. 293–296.

[12] Micropelt, Thermogenerators, 2016. [Online]. Available: http://www.micropelt.com/thermogenerator.php.

[13] H.G. Lee, N. Chang, Powering the IoT: Storage-less and converter-less energy harvesting, in: Proceedings of the IEEE/ACM Asia and South Pacific Design Automation Conference, 2015, pp. 124–129.

[14] C. Lu, S.P. Park, V. Raghunathan, K. Roy, Efficient power conversion for ultra low voltage micro scale energy transducers, in: Proceedings of the IEEE Design, Automation, and Test Conference in Europe, 2010, pp. 1602–1607.

[15] K. Wasa, T. Matsushima, H. Adachi, I. Kanno, H. Kotera, Thin-film piezoelectric materials for a better energy harvesting MEMS, J. Microelectromech. Syst. 21 (2) (2012) 451–457.

[16] A.L. Betz, R.T. Boreiko, Space applications for HgCdTe at FIR wavelengths between 50 and 150 μm, in: Proceedings of the SPIE Materials for Infrared Detectors, 2001, pp. 1–9.

[17] Y.T. Hsieh, C.L. Fang, C.F. Su, H.H. Tsai, Y.Z. Juang, A hybrid ambient energy harvesting integrated chip (IC) for the Internet of Things (IoT) and Portable Applications, in: Proceedings of the IEEE International Conference on Electrical Machines and Systems, 2016, pp. 1–4.

[18] R. Buzilo, B. Likhterov, R. Giterman, I. Levi, A. Fish, A. Belenky, Approach to integrated energy harvesting voltage source based on novel active TEG array system, in: Proceedings of the IEEE Faible Tension Faible Consommation, 2014, pp. 1–4.

[19] I. Vaisband, M. Saadat, B. Murmann, A closed-loop reconfigurable switched-capacitor DC-DC converter for sub-mW energy harvesting applications, IEEE Trans. Circuits Syst. I. Regul. Pap. 62 (2) (2015) 385–394.

[20] B. Song, K.S. Moon, C.P. Wong, Recent developments in design and fabrication of graphene-based interdigital micro-supercapacitors for miniaturized energy storage devices, IEEE Trans. Compon. Hybrids Manuf. Technol. 6 (12) (2016) 1752–1765.

[21] X.D. Do, H.H. Nguyen, S.K. Han, D.S. Ha, S.G. Lee, A self-powered high-efficiency rectifier with automatic resetting of transducer capacitance in piezoelectric energy harvesting systems, IEEE Trans. Very Large Scale Integr. (VLSI) Syst. 23 (3) (2015) 444–453.

[22] S. Ghosh, H.T. Wang, W.D. Leon-Salas, A circuit for energy harvesting using on-chip solar cells, IEEE Trans. Power Electron. 29 (9) (2014) 4658–4671.

[23] N. Weissman, S. Jameson, E. Socher, W-band CMOS on-chip energy harvester and rectenna, in: Proceedings of the IEEE International Microwave Symposium, 2014, pp. 1–3.

[24] K.Y. Lee, D. Brown, S. Kumar, Silicon nanowire arrays based on-chip thermoelectric generators, IEEE Trans. Compon. Hybrids Manuf. Technol. 5 (8) (2015) 1100–1107.

[25] B. Martinez, M. Montón, I. Vilajosana, J.D. Prades, The power of models: Modeling power consumption for IoT devices, IEEE Sens. J. 15 (10) (2015) 577–5789.

Boris Vaisband was born in November, 1983 in Moscow, Russia. He is currently a postdoctoral scholar at the University of California, Los Angeles, working on wafer level heterogeneous systems integration. He received a B.Sc. degree in Computer Engineering from the Technion-Israel Institute of Technology, Haifa, Israel in 2011, and a M.S. and Ph.D. degrees in Electrical Engineering from the University of Rochester, Rochester, NY, in, respectively 2012 and 2017. Between 2008 and 2011, he held a hardware design position at Intel Corporation in Israel. In the summer of 2013, he interned with the Optical and RF research group at Cisco Systems Inc., San Jose, CA. In the summer of 2015, he interned with the Power Design team at Google Inc., Mountain View, CA. His current research interests include integration of heterogeneous systems, power delivery, thermal aware design and floorplanning, and noise coupling.

Eby G. Friedman received the B.S. degree from Lafayette College in 1979, and the M.S. and Ph.D. degrees from the University of California, Irvine, in 1981 and 1989, respectively, all in electrical engineering.

From 1979 to 1991, he was with Hughes Aircraft Company, rising to the position of manager of the Signal Processing Design and Test Department, responsible for the design and test of high performance digital and analog IC's. He has been with the Department of Electrical and Computer Engineering at the University of Rochester since 1991, where he is a Distinguished Professor, and the Director of the High Performance VLSI/IC Design and Analysis Laboratory. He is also a Visiting Professor at the Technion-Israel Institute of Technology. His current research and teaching interests are in high performance synchronous digital and mixed-signal microelectronic design and analysis with application to high speed portable processors and low power wireless communications.

He is the author of over 400 papers and book chapters, 12 patents, and the author or editor of 16 books in the fields of high speed and low power CMOS design techniques, 3-D design methodologies, high speed interconnect, and the theory and application of synchronous clock and power distribution networks. Dr. Friedman is the Editor-in-Chief of the *Microelectronics Journal*, a Member of the editorial boards of the *Analog Integrated Circuits and Signal Processing*, *Journal of Low Power Electronics*, and *Journal of Low Power Electronics and Applications*, Chair of the *IEEE Transactions on Very Large Scale Integration (VLSI) Systems* steering committee, and a Member of the technical program committee of numerous conferences. He previously was the Editor-in-Chief of the *IEEE Transactions on Very Large Scale Integration (VLSI) Systems*, the Regional Editor of the *Journal of Circuits, Systems and Computers*, a Member of the editorial board of the *Proceedings of the IEEE, IEEE Transactions on Circuits and Systems II: Analog and Digital Signal Processing, IEEE Journal on Emerging and Selected Topics in Circuits and Systems*, and *Journal of Signal Processing Systems,* a Member of the Circuits and Systems (CAS) Society Board of Governors, Program and Technical chair of several IEEE conferences, and a recipient of the IEEE Circuits and Systems 2013 Charles A. Desoer Technical Achievement Award, a University of Rochester Graduate Teaching Award, and a College of Engineering Teaching Excellence Award. Dr. Friedman is a Senior Fulbright Fellow and an IEEE Fellow.